Journal of Geoscience and Environment Protection, 2025, 13(6), 264-274
https://www.scirp.org/journal/gep
ISSN Online: 2327-4344
ISSN Print: 2327-4336

Characterization of Canyon Wall Slump and Its Impact on Infilling of the Central Canyon in Qiongdongnan Basin

Da Li[1], Qianqian Tao[1], Pan Yang[2]

[1]CNOOC China Ltd._Hainan, Haikou, China
[2]Optical Science and Technology (Chengdu) Ltd., Chengdu, China
Email: y1458651011@foxmail.com

How to cite this paper: Li, D., Tao, Q. Q., & Yang, P. (2025). Characterization of Canyon Wall Slump and Its Impact on Infilling of the Central Canyon in Qiongdongnan Basin. *Journal of Geoscience and Environment Protection, 13,* 264-274.
https://doi.org/10.4236/gep.2025.136018

Received: May 12, 2025
Accepted: June 24, 2025
Published: June 27, 2025

Abstract

Objectives: Mass transport deposits (MTDs) often have a certain control effect on the development of river channels and the transformation of topography and geomorphology. **Methods:** In order to explore the influence of MTDs in waterways, this paper, based on three-dimensional seismic data of the west section of the Central canyon in Qiongdongnan Basin, conducted a detailed characterization of the canyon wall collapse phenomenon and block transport sedimentary system in the study area. The geological model of canyon wall collapse was constructed by using fluid dynamics software Fluent to explore the sedimentary distribution and influence of canyon wall collapse. **Results and Conclusions:** The results show that: 1) The study area is located on the west side of the Central canyon, and large-scale erosion scratches have developed inside the canyon, and compressive ridges and thrust fault structures have been identified; 2) Large-scale erosion scratches occurre in the northern part of the study area, which can be interpreted as the collapse of the canyon wall due to the instability of the target layer. Large-scale bulk transport sediments developed in the target layer eroded the underlying layer and destroyed the original sediments, but the sediments provided a certain provenance basis for the canyon filling; 3) Through the forward modeling of canyon wall collapse, it is found that both sides of the canyon have different erosion degrees, and the steep side of the canyon wall is prone to slide. With the completion of the filling of the canyon, the limit of the channel is weakened, and it is easier to form a migration channel.

Keywords

Central Canyon, Mass Transport Deposit, Thrust Fault, Compression Ridge

1. Introduction

The mass transport deposit (MTDs) is an important geomorphic unit of deep-water seafloor, which has always been of great concern to scholars at home and abroad. (Kneller et al., 2016) argue that the sedimentation of large MTDs reshapes the seafloor topography of continental slopes and uplifts, and the undulating terrain at the top of MTDs creates extensive potential for stratigraphic traps. The location and geometric shape of this stratigraphic trap are influenced by the interaction between turbidity currents and topography. (Gong et al., 2022) believe that the uneven top surface of MTDs has a certain impact on subsequent sedimentation. The greater the degree of undulation, the more favorable it is for sediment unloading, thus forming a larger-scale submarine fan. (Su et al., 2014) believe that in the northern part of the central canyon in the Qiongdongnan Basin, MTDs account for a very large proportion of the provenance, and the MTDs in local areas have strong hydrodynamic conditions, which provide conditions for transforming the shape of the canyon. At the same time, research on the causes of canyon wall collapse is constantly advancing. (Stephen et al., 2022) believe that the collapse of canyon walls in his study area is related to the high precipitation at that time, and abundant water supply will penetrate the canyon walls and cause collapse; However, Nasif et al. believe that the steep slope of the canyon and geological tectonic activity lead to large-scale block transport of local canyon walls. Li Ling speculated that the conditions for the collapse of a waterway are not only related to the inclination angle of the waterway wall, but also to the continuous accumulation of sediment from the source of the landslide point embankment. With the evolution of fluid simulation software, in recent years, the use of numerical simulation methods to study the distribution of turbidity current sedimentation has attracted the attention of scholars. Among them, Wang Y. et al. simulated and studied the flow and sedimentation characteristics of turbidity currents with different inflow mechanisms based on the Reynolds averaged Navier Stokes equation and RANS turbulence model. (Yang, 2020) used the FLOW 3D software to conduct numerical simulations of turbidity current sedimentation characteristics by controlling factors such as particle size, slope, and inflow mechanism. Zeng et al. used a layered average three-equation flow model to study the influence of sediment properties on turbidity current flow and sedimentary morphology. In the process of numerical simulation, the results showed a good agreement with the turbidity current discovered in the study, which verified the feasibility of numerical simulation of turbidity current.

Previous researchers often focused on the causes and impacts of continental slope landslides, with little detailed characterization and forward modeling of canyon wall landslides. This article is based on three-dimensional seismic data from the western part of the central canyon in the Qiongdongnan Basin, identifying the typical geomorphic features of canyon wall collapse. The fluid software Fluent is used to simulate and analyze the canyon wall collapse, revealing the process and subsequent effects of canyon wall collapse. Simulation results with geological prototypes are obtained to further determine the causes and impact of canyon wall collapse in the study area, providing a certain geological understanding for oil and gas exploration in the central canyon area of the Qiongdongnan Basin.

2. Geological Overview

The Qiongdongnan Basin is located at the intersection of three major tectonic plates (the Eurasian Plate, the Pacific Plate, and the Indochinese Plate), on the northern continental margin of the South China Sea (Su et al., 2013). The basin covers an area of approximately 4.5 × 104 km^2 and is distributed in a NE direction. The basin has a structural pattern of north-south zoning and east-west block division, consisting of four primary structural units from north to south: the northern depression zone, the central uplift zone, the central depression zone, and the southern uplift zone (Xu et al., 2012; Wang et al., 2014) (**Figure 1**). The basin has gone through four stages of structural evolution, including faulting, subsidence, thermal subsidence, and accelerated subsidence. The study area is currently in the accelerated subsidence stage (Zhang, 2020; Lei et al., 2011) (**Figure 1**). Due to the influence of the Honghe and Hainan Island sources, the development of the Central Canyon exhibits a "multi-stage and multiple" characteristic. In the early stage, the source on the west side of the canyon played a dominant role, while in the late stage, it was mainly influenced by the source from Hainan Island (Li et al., 2023, Zhang et al., 2017). The research area is located in the Yinggehai Formation of the Lingshui Depression in the central canyon of the Qiondongnan Basin, with a water depth of several hundred to several thousand meters. The canyon has developed various sedimentary units such as block transport sediments (MTDs), embankment sediments, and bottom retention sediments (Sun et al., 2022). This article focuses on the study of block transport sedimentary systems.

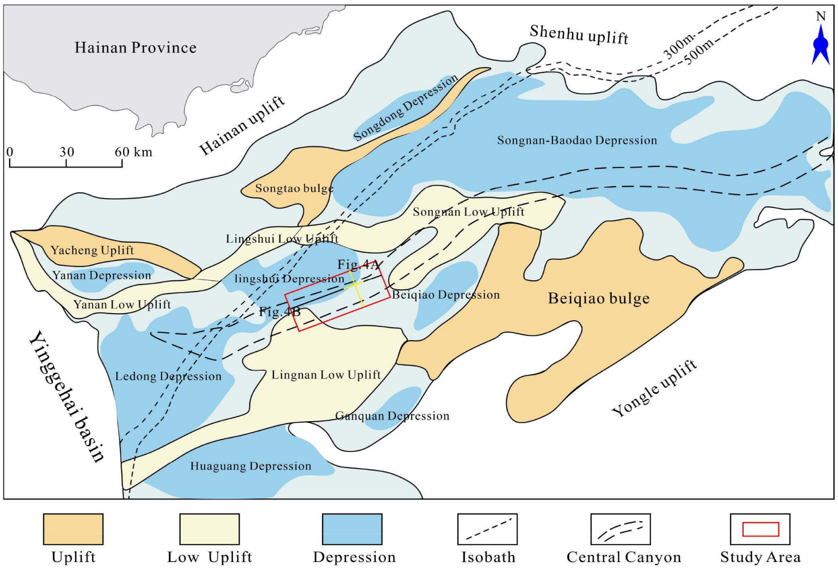

Figure 1. Location of research area and brief table of stratigraphic sequence.

3. Identification of Canyon Wall Slump

From the attribute map (**Figure 2**) and the three-dimensional topographic map (**Figure 3**), it can be seen that during this period, not only waterways were developed, but also large-scale block transport sediments were developed in the northern part of the study area. The seismic facies were mainly characterized by chaotic reflections, interbedded sub parallel reflections, and poor continuity of the same phase axis. Large-scale block transport and sedimentation are carried downwards along the canyon walls, and there are obvious strip-shaped erosion scratches on the profile maps (**Figure 4(A)**, **Figure 4(B)**), as well as the development of thrust faults and compression ridges, presenting an undulating bottom interface. In the attribute map, the large area of erosion scratches caused by MTDs is clearly represented by parallel stripes at the rear end of the MTD propulsion direction (**Figure 2**, **Figure 4(A)**), with few parallel stripes visible at the front end. This is explained as a strong amplitude reflection feature caused by sediment accumulation due to resistance during the MTD sliding process. From the topographic map of the study area (**Figure 3**), it can be seen that the northern boundary of the canyon basically disappeared during this period. The canyon is filled with MTDs coming from the north and northwest directions, and there is also a clear elongated negative terrain in the northern part of the canyon, which is explained by the erosion scratches formed by the collapse of MTDs, which corresponds to the attribute map (**Figure 2**).

3.1. Compression Ridge

The geometric shape of compression ridges is easily recognizable in profiles, and

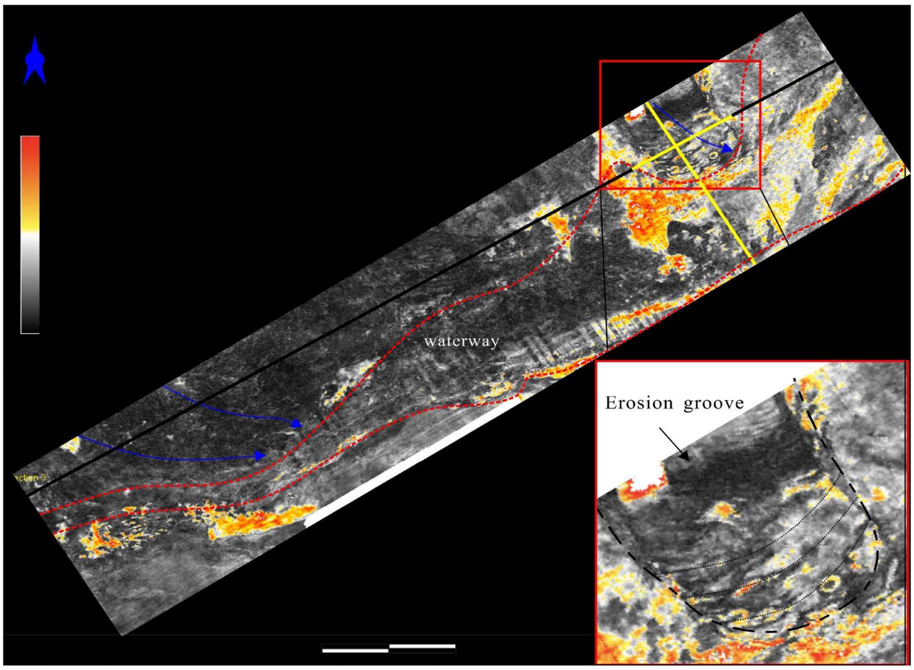

Figure 2. Root-mean-square attribute diagram of the research area.

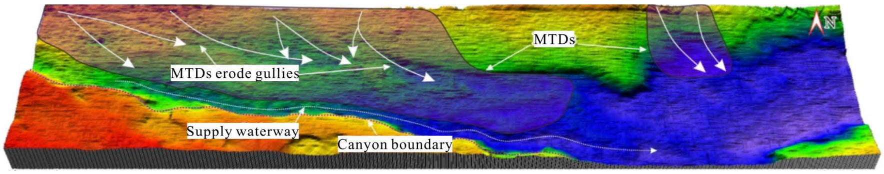

Figure 3. Canyon geomorphology map of the study area.

thrust faults often appear simultaneously with compression ridges, forming a series of raised peaks and depressed valleys that alternate between peaks and valleys. The seismic profile shows strong amplitude reflection characteristics (**Figure 4(A)**). Squeezing ridges are widely developed in the toe area due to the downward transport of gravity flow sediments. Most sediments accumulate at the toe to form thrust faults, and under certain slope conditions, the accumulation of sediments at the toe can also form a certain scale of squeezing ridges, which are commonly developed in block transport in deep water and on land (He et al., 2018). The development of thrust faults causes uneven terrain and is a favorable area for turbidity current deposition unloading.

3.2. Erosion Groove

The bottom interface is a weak surface formed by MTDs under the action of gravity, generally with good continuity. During the process of gravity flow sedimentation moving downwards along the bottom interface, due to the varying degrees of resistance, consolidation ability at different locations, and erosion resistance of the bottom interface, the bottom interface will be damaged by sediments, forming erosion scratches. The concave part of the damaged bottom interface is called an erosion groove (**Figure 4(B)**). The width of the erosion groove discovered in the research area is up to 3 km. The upper part of the erosion scratch often develops structures such as thrust faults, and the distribution of erosion grooves at the bottom interface can be clearly seen through the RMS property map. There are two reasons for their formation: 1) erosion of underlying strata by high-speed fluids; 2) The floating blocks carried by high-speed fluids jump forward, causing erosion of the bottom strata (Qin, 2012).

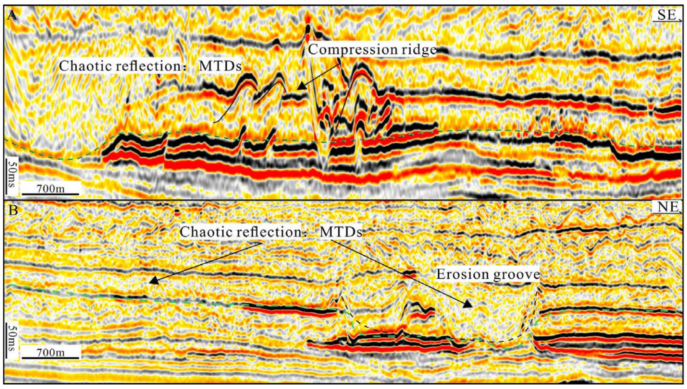

Figure 4. Typical seismic profile of the study area.

4. Models and Methods

In recent years, with the continuous development of computer technology, many unique numerical simulation softwares have emerged on the market, such as Flow 3D, Fluent, Phoenics, CFX, etc. Each software has a different focus on simulation. Fluent software has the ability to simulate a wide range of physical phenomena such as flow, turbulence, heat transfer, and reactions. Due to its high degree of visualization, rich physical models, advanced numerical methods, and powerful pre-processing and post-processing capabilities, this software has a wide range of applications in aerospace, oil and gas, water conservancy, and other fields (Liu, 2019).

The numerical calculation of Fluent multiphase flow model mainly includes Euler Euler method and Euler Lagrange method. Due to the fact that the volume fraction of the dispersed phase set in the Euler Lagrange method cannot exceed 10%, while the Euler Euler method can accept particles with larger volume fractions, this paper chooses the Euler Euler method (Jiang et al., 2005). There are three types of multiphase flow models in Fluent, namely VOF (Free Surface Tracking) model, Mixture model, and Euler model. The scenarios applied by each model are different (**Table 1**).

Table 1. Multiphase flow model selection table.

Application Scenarios	Model Selection
Bubble, droplet, or particle-laden flow with dispersed phase volume < 10%	Discrete Phase Model (DPM)
Stratified flow/free surface flow	Volume of Fluid (VOF) Model
Slurry flow, hydraulic transport, flow with mixing/separation	Eulerian/Mixture Model
Sediment settlement	Eulerian Model

4.1. Grid Construction and Parameter Setting

1) Volume fraction equation:

Based on the Euler two-phase flow simulation used in the article, the two phases are considered as interpenetrating continuum, therefore, a volume fraction is required to represent the space occupied by each phase in the control volume. The volume occupied by the *q*-th phase is defined as:

$$V_q = \int_V \alpha_q \mathrm{d}V \tag{1}$$

The total volume fraction of two different phases is 1:

$$\sum_{q=1}^{n} \alpha_q = 1 \tag{2}$$

Therefore, the effective density of the *q*-th phase: $\hat{\rho}_q = \alpha_q \rho_q$ In the equation, *α_q* is the volume fraction of the *q*-phase, and at the same time, the Euler model shares a common pressure value (Zeng et al., 1997).

2) Continuity equation:

The Euler method is to take any fluid contained in a control body (or control element) as the research object in a space filled with fluid particles. For a certain control body, the law of conservation of mass can be expressed as: the increase in fluid mass in the control body per unit time = ∑[the mass of fluid flowing into the control body per unit time − ∑the mass of fluid flowing out of the control body per unit time]. Therefore, the continuity equation for the q-th phase is (Hu et al., 2022):

$$\frac{\partial}{\partial t}\left(\alpha_q \rho_q\right)+\nabla\cdot\left(\alpha_q \rho_q \vec{v}_q\right)=\sum_{p=1}^{n}\left(\dot{m}_{pq}-\dot{m}_{qp}\right)+S_p \tag{3}$$

($\dot{m}_{pq}$: transfer from the p-th phase to the q-th phase; $\dot{m}_{qp}$: transfer from the q-th phase to the p-th phase; S_p : Source item, default is 0; $\vec{V}_q$: velocity of the q-th phase.)

3) Momentum conservation equation:

Any flow problem must satisfy the law of conservation. According to Newton's second law, write the momentum change of the q-th phase in the control body: the rate of change of momentum over time + the momentum change caused by the fluid passing through the surface of the control body = the force acting on that phase in the control body [26]. The momentum equation is:

$$\begin{aligned}&\frac{\partial}{\partial t}\left(\alpha_q \rho_q \vec{v}_q\right)+\nabla\cdot\left(\alpha_q \rho_q \vec{v}_q \vec{v}_q\right)\\&=-\alpha_q \nabla p+\nabla\cdot\bar{\bar{\tau}}_q+\alpha_q \rho_q \vec{g}+\sum_{p=1}^{n}\left(\vec{R}_{pq}+\dot{m}_{pq}\vec{v}_{pq}-\dot{m}_{pq}\vec{v}_{pq}\right)+\left(\vec{F}_q+\vec{F}_{lift,q}+\vec{F}_{vm,q}\right)\end{aligned} \tag{4}$$

($\bar{\bar{\tau}}_q$: stage stress of phase q; $\vec{g}$: gravitational acceleration; $\vec{F}_q$: volume force; $\vec{F}_{lift,q}$: lift force; $\vec{F}_{vm,q}$: virtual mass force; $\vec{R}_{pq}$: the interaction force between phases; v_{pq} : Interphase velocity.)

4.2. Geometric Structure and Boundary Conditions

The professional modeling software for geometric structures on the market includes CAD, Solid Works, etc. However, considering software compatibility issues and subsequent secondary modifications, Fluent's built-in Space Claim component is used. Open this component and based on the principle of geometric similarity, while ensuring the same Froude number (Fr = V/√ gl), set the scale of the 2D model to 1:1000 and create a rectangle with a length of 30 m and a width of 18 m. Divide the model into two regions, Flow up and Flow down, and establish a mesh model of the canyon wall (**Figure 5**). After establishing the geometric model proportionally in Space Claim, import it into the mesh for mesh partitioning, set the mesh density to 2 mm × 2 mm, and have a total of 72,585 nodes (65,344 elements).

4.3. Setting and Solving Initial Conditions

The collapse of canyon walls is often closely related to various factors such as

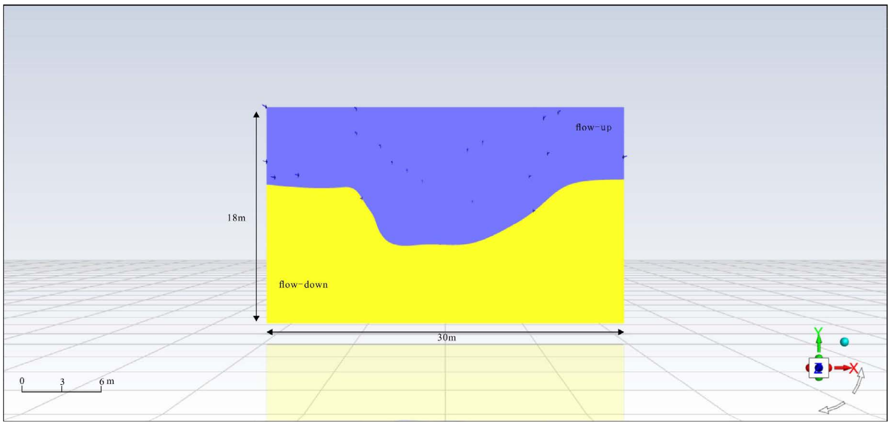

Figure 5. Grid diagram of slump model.

sediment accumulation, heavy precipitation, and geological activity. In order to better explore the dynamic response of canyon wall collapse, this paper sets up a transverse waterway model of canyon wall collapse (**Figure 5**). In order to observe the process of canyon wall collapse more intuitively, the canyon wall collapse model is simplified. The initial left and right slopes of the canyon wall are set differently, with the left wall steep and the right wall gentle.

In the general setting, we use transient simulation to observe the sedimentary distribution of turbidity currents. After the control equation is discretized, it can be solved. Here, the pressure velocity coupling scheme uses the most widely used flow field calculation method, implicit SIMPLE algorithm, which is mainly used for prediction and adjustment to achieve convergence faster. In order to make the turbidity current sedimentation process more complete, the iteration number is uniformly set to 200 steps, and the step size is set to 0.1. Add water and sand to the material (where sand refers to turbidity particles, specific parameters are set in **Table 2**, refer to Wang Yue's [9] settings for turbidity particle size and related parameters). Set up solid-liquid mixing inflow at the entrance.

Table 2. Multiphase flow model selection table.

Parameter Name	Set Value
Turbidity Current Initial Velocity (m/s)	1
Particle Diameter (mm)	0.04 (Silt)
Particle Density (g/cm^3)	2650 (Silt)
Gravitational Acceleration (m/s^2)	−9.81

5. Simulation Results and Discussion

This article simulates the instability and collapse of the canyon wall caused by the cutting of the canyon wall by the waterway. Observing the sand cloud map of the flow in **Figure 6**, it is not difficult to find that the sediment in the waterway gradually erodes the canyon wall, leading to the collapse of the northern canyon wall.

As the canyon wall continues to collapse, a part of the river channel is filled.

Figure 6 shows the final stage of canyon wall collapse. When turbidity currents are transported in the canyon, they erode the canyon walls, leading to a decrease in the consolidation degree of the canyon base, instability of the canyon walls, and collapse. There is a small amount of canyon wall collapse sediments in the waterway, and a large number of block transport sediments have developed in the target layer, providing a certain source of material for canyon filling. MTDs have a strong effect on the alteration of underlying sedimentary layers (Figure 6). On the north side of the eastern section of the canyon in the research area, MTDs have caused serious damage to the underlying strata. There are approximately parallel stripes arranged on the north side of the eastern section of the canyon, which are generally perpendicular to the direction of MTDs advancement (Figure 7). On the seismic profile, it can be seen that the thrust fault cuts through the underlying strata, causing the strata to be broken and the connectivity of the sand body to deteriorate. The strata will also be mixed with collapsed MTDs, resulting in increased heterogeneity of the lithology of the strata (Figure 4(A), Figure 4(B)). According to the different lithological compositions, MTDs play a role in local or regional sealing by eroding the underlying strata, and are likely to serve as reservoirs or cap rocks, providing a certain direction for oil and gas exploration.

As turbidity currents continue to erode the canyon walls, it was observed that there are developed thrust faults within the MTDs formed by the simulation results (Figure 6). These thrust faults can cause uneven top interfaces, affecting the subsequent sedimentary distribution of turbidity currents. The development direction of the compression ridges in the pattern diagram is parallel to the direction of collapse, which is formed by the accumulation of resistance at the toe (Figure 7). The MTDs formed by the deposition and collapse of the developed block flow are also clearly visible in the direction of the attribute map (Figure 2) and the topographic map (Figure 3), and are transported downwards in the direction perpendicular to the arrangement of the compression ridges.

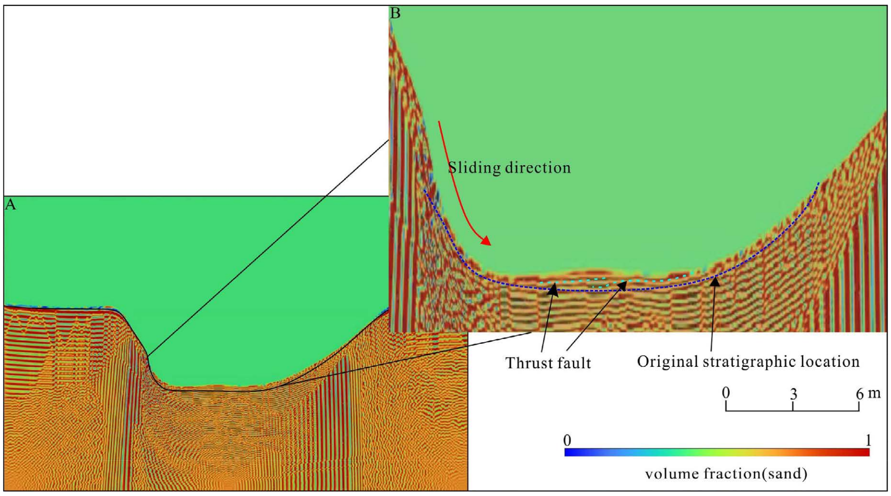

Figure 6. Cloud image at the end of slump simulation.

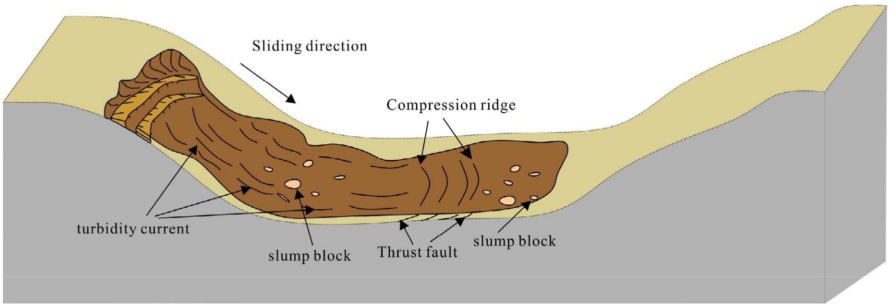

Figure 7. Slide mode diagram.

6. Conclusion

This article is based on three-dimensional seismic data of the western section of the central canyon in the Qiongdongnan Basin, and finely depicts the phenomenon of canyon wall collapse in the study area. Using fluid mechanics software Fluent, a canyon wall model was constructed to realize the sedimentation process and distribution of canyon wall collapse. The results show that:

1) The research area is located on the west side of the Central Canyon, where large-scale erosion scratches have developed and compression ridges and thrust fault structures have been identified.

2) A large-scale erosion scratch occurred in the northern part of the research area, which is explained by the instability and collapse of the canyon wall. The target layer developed large-scale block transport sedimentation, which eroded the underlying strata and caused damage to the original sediments. However, this sedimentation provided a certain source basis for canyon filling.

3) Through forward simulation of canyon wall collapse, it was found that there are different degrees of erosion on both sides of the canyon, and the steep side of the canyon wall is prone to collapse.

Conflicts of Interest

The authors declare no conflicts of interest regarding the publication of this paper.

References

Gong, G. C., Li, L., He, W. et al. (2022). Numerical Simulation of Post-Mass Transport Deposition: A Case Study of the Margin Slope of South China Sea. *Marine Geology Frontiers, 38,* 75-83.

He, Y. L., Kuang, Z. G., & Xu, M. J. (2018). Seismic Reflection Characteristics and Genetic Mechanism of Quaternary Block Transport Sediments in Beikang Basin. *Geological Science and Technology Information, 37,* 258-268.

Hu, H. L. (2022). *Numerical Simulation and Optimization of CMCBR Based on Fluent.* Nanchang University.

Jiang, T., Xie, X. O., & Tang, S. L. (2005). Hydrodynamic Simulation of Turbidity and Its Application for Reservoir Prediction. *Bulletin of Geological Science and Technology, 2,* 1-6.

Kneller, B., Dykstra, M., Fairweather, L., & Pablo, J. (2016). Mass-Transport and Slope Accommodation: Implications for Turbidite Sandstone Reservoirs. *AAPG Bulletin, 100,* 213-235.

Lei, C., Ren, J. Y., Li. X. S. et al. (2011). Structural Characteristics and Petroleum Exploration Potential in the Deep-Water Area of the Qiongdongnan Basin, South China Sea. *Petroleum Exploration and Development, 38,* 560-569.

Li, D., Xu, Q., Wang, Y. F. et al. (2013). Provenance Analysis of the Pliocene Central Canyon in Qiongdongnan Basin and Its Implications. *Oil Geophysical Prospecting, 48,* 799-803+674-675+854.

Li, L., Li, L., Yan, H. M. et al. (2023). 3D Seismic Characterization and Origination of Gravity Flow Geomorphic Units on Continental Slope: A Case Study of Lingshui Sag, Qiongdongnan Basin. *Marine Geology & Quaternary Geology, 43,* 37-48.

Liu, B. (2019). *Fluent19.0 Fluid Simulation from Beginner to Proficient*. Tsinghua University Press.

Qin, Z. L. (2012). *Sedimentary Process, Distribution and Mechanism of Mass Transport Deposits, the Slope Area of Northern South China Sea*. Graduate School of Chinese Academy of Sciences (Institute of Oceanography).

Stephen, S., Noah, R., E. et al. (2022). Exposed Columns in the Valles Caldera Ignimbrites as Records of Hydrothermal Cooling, Jemez Mountains, New Mexico, USA. *Journal of Volcanology and Geothermal Research, 426,* Article 107536.

Su, M., Xie, X. O., Wang, Z. F. et al. (2013). Sedimentary Evolution of Central Canyon System in Qiongdongnan Basin, Northern South China Sea. *Acta Petrolei Sinica, 34,* 467-478.

Su, M., Zhang, C., Xie, X. O. et al. (2014). Analysis of Controlling Factors of Deep Water Canyon System: A Case Study of Central Canyon System in Qiongdongnan Basin, Northern South China Sea. *Science in China: Earth Sciences, 44,* 1807-1820.

Sun, H. X., Li, L., Ding, S. et al. (2022). Sedimentary Architecture of the Central Canyon in L Area of Qiongdongnan Basin and Their Evolution and Controlling Factors. *Marine Geology Frontiers, 38,* 61-71.

Wang, Z. S., Liu, Z., Sun, Z. P. et al. (2014). Preliminary Prediction and Evaluation of Oligocene Source Rocks in Ledong-Lingshui Sag in Deep-Water Area of Qiongdongnan Basin. *Journal of Central South University (Science and Technology), 45,* 876-888.

Xu, H. Z., Cai, D. S., Sun, Z. P. et al. (2012). Filling Characters of Central Submarine Canyon of Qiongdongnan Basin and Its Significance of Petroleum Geology. *Acta Geologica Sinica, 86,* 641-650.

Yang, Y. P. (2020). *Numerical Simulation of Turbidity Currents Based on Flow3D*. Harbin Institute of Technology.

Zeng, J. J., & Lowe, D. R. (1997). Numerical Simulation of Turbidity Current Flow and Sedimentation: I. Theory. *Sedimentology, 44,* Article 84.

Zhang, D. J., Zhang, Y. Z., Shao, L. et al. (2017). Sedimentary Provenance in the Central Canyon of Qiongdongnan Basin in the Northern South China Sea. *Natural Gas Geoscience, 28,* 1574-1581.

Zhang, P. (2020). *Study on Shelf-Slope Evolution and Sedimentary System of Neogene in North South China Sea*. Xi’an Shiyou University.